Mühendislik Bilimleri ve Tasarım Dergisi
14(1), 191-202, 2026
e-ISSN: 1308-6693

Journal of Engineering Sciences and Design
DOI: 10.21923/jesd.1880712

Araştırma Makalesi Research Article

# ADDITIVELY MANUFACTURED REFLECTOR-BACKED SUB-6 GHZ BOW-TIE ANTENNA

**Burak DÖKMETAŞ[1*]**

[1]Kafkas University, Department of Electrical and Electronics Engineering, 36000 Kars, Türkiye

**Keywords**

*Bow-tie Antenna, Sub-6 GHz, Wideband, Additive Manufacturing, Antenna Gain.*

**Abstract**

This study presents a gain enhanced bow-tie antenna operating in the lower portion of the sub-6 GHz frequency spectrum, which is of interest for broadband wireless and sensing applications. The proposed antenna is based on a crossed geometry formed by nested equilateral triangular elements symmetrically arranged on both sides of a dielectric substrate, enabling multiple effective current paths and wide impedance bandwidth without the need for complex matching networks. The antenna is fabricated using fused deposition modeling (FDM) technology with PREPERM ABS800 filament. To enhance the realized gain, a dielectric-backed reflector incorporating a conductive layer is integrated beneath the radiating structure and mechanically supported by four dielectric posts. Experimental measurements show that the proposed antenna covers a measured bandwidth from 1.2 GHz to 3.1 GHz, resulting in an absolute bandwidth of 1.9 GHz. The results further indicate that the inclusion of the reflector provides a clear realized gain enhancement across the operating band, increasing the gain from approximately 2.6–3.7 dBi to about 4.5–5.7 dBi. These results confirm that the proposed design offers a fabrication friendly, and broadband antenna solution with consistent gain enhancement, making it suitable for lower sub-6 GHz wireless and sensing systems.

# EKLEMELİ İMALAT YÖNTEMİYLE ÜRETİLEN REFLEKTÖR DESTEKLİ SUB-6 GHZ BOW-TIE ANTEN

**Anahtar Kelimeler**

*Bow-tie Anten, Sub-6 GHz, Genişbant, Eklemeli İmalat, Anten Kazancı.*

**Öz**

Bu çalışma, alt sub-6 GHz frekans spektrumunun alt kısmında çalışan, kazancı artırılmış bow-tie anten tasarımını sunmaktadır. Bu frekans aralığı, geniş bant kablosuz haberleşme ve algılama uygulamaları açısından önemlidir. Önerilen anten, bir dielektrik altlık üzerinde her iki tarafta simetrik olarak yerleştirilmiş, iç içe geçmiş eşkenar üçgensel elemanlardan oluşan çapraz bir geometriye sahiptir. Bu yapı, karmaşık empedans eşleme ağlarına ihtiyaç duymadan birden fazla etkin akım yolu oluşturarak geniş bir empedans bant genişliği elde edilmesini sağlamaktadır. Anten, ergiterek yığma modeli (FDM) tabanlı 3B yazıcı kullanılarak PREPERM ABS800 filament ile üretilmiştir. Gerçeklenen kazancı artırmak amacıyla, iletken bir katman içeren dielektrik destekli bir reflektör, ışıyıcı yapının altına entegre edilmiş ve dört adet dielektrik destek ayağı ile mekanik olarak sabitlenmiştir. Deneysel ölçümler, antenin 1.2-3.1 GHz arasında çalıştığını ve 1.9 GHz'lik mutlak bant genişliği sunduğunu göstermektedir. Sonuçlar reflektörün eklenmesiyle kazancın yaklaşık 2.6–3.7 dBi seviyelerinden 4.5–5.7 dBi aralığına yükseldiğini ortaya koymaktadır. Elde edilen sonuçlar, önerilen tasarımın üretimi kolay, geniş bantlı ve tutarlı kazanç artışı sunan bir anten çözümü olduğunu göstermektedir.

**Cite**

Dökmetaş, B., (2026). Additively Manufactured Reflector-Backed Sub-6 Ghz Bow-Tie Antenna, Journal of Engineering Science and Design, 14(1), 191-202.

**Author ID (ORCID Number)**

B. Dokmetas, 0000-0001-5900-6691

**Makale Süreci / Article Process**

| | |
|---|---|
| **Başvuru Tarihi / Submission Date** | 03.02.2026 |
| **Revizyon Tarihi / Revision Date** | 11.02.2026 |
| **Kabul Tarihi / Accepted Date** | 26.02.2026 |
| **Yayım Tarihi / Published Date** | 20.03.2026 |

[*] İlgili yazar / Corresponding Author: burakd@kafkas.edu.tr, +90 530 834 12 35

# ADDITIVELY MANUFACTURED REFLECTOR-BACKED SUB-6 GHZ BOW-TIE ANTENNA

Burak DOKMETAS[1†]
[1]Kafkas University, Department of Electrical and Electronics Engineering, 36000 Kars, Türkiye

## Highlights

- A gain-improved wideband bow-tie antenna is presented for sub-6 GHz operation.
- 3D-printed dielectric-backed reflector is used to enhance broadband gain.
- Measured results confirm the simulation outcomes.

## Graphical Abstract

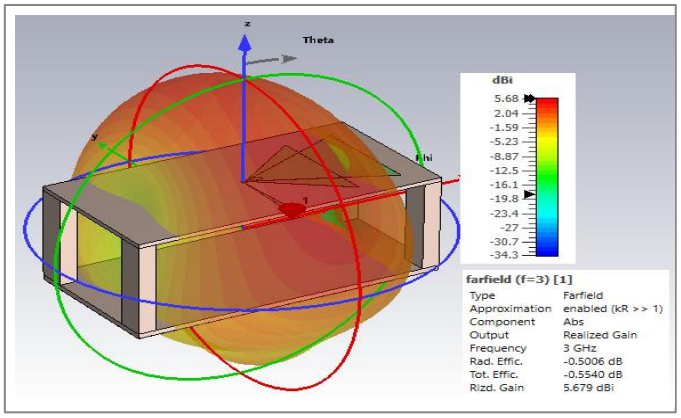


**Figure.** 3D radiation patterns of the proposed bow-tie antenna with reflector

## Purpose and Scope

This study aims to design and experimentally validate a wideband bow-tie antenna with improved gain performance for wireless and sensing applications. The work demonstrates how a reflector can be practically integrated into an antenna using the fabrication flexibility of 3D printing, and experimentally verifies broadband operation and gain enhancement through, additively manufactured dielectric reflector.

## Design/methodology/approach

The proposed antenna employs a crossed bow-tie geometry formed by nested equilateral triangular elements and is fabricated using PREPERM ABS800 dielectric filament at a controlled infill ratio. A dielectric-backed reflector is integrated to enhance radiation performance, and the design is validated through full-wave simulations and experimental measurements.

## Findings

The proposed bow-tie antenna achieves wide impedance bandwidth across the sub-6 GHz band. Measurement results confirm consistent gain improvement with good agreement between simulations and experiments.

## Research limitations/implications

The study is limited to a single-element bow-tie antenna. Future work may extend the proposed approach to array and explore further optimization enabled by additive manufacturing.

## Orginality

This study presents a wideband bow-tie antenna with improved gain achieved through the practical integration of a 3D-printed dielectric reflector. The originality lies in demonstrating a fabrication-friendly reflector implementation using a state-of-the-art RF-optimized material, experimentally validating its effectiveness for sub-6 GHz applications. The proposed approach offers a simple and scalable solution enabled by additive manufacturing.

† Corresponding Author: burakd@kafkas.edu.tr, +90 530 834 12 35

## 1. Introduction

The rapid growth of modern wireless communication systems has significantly increased the demand for wideband antennas capable of operating over the sub-6 GHz frequency spectrum. This band has gained particular importance due to its favorable propagation characteristics, wide coverage, and relatively low penetration losses, making it a key enabler for contemporary wireless platforms such as sub-6 GHz 5G, wireless local area networks (WLAN), Internet of Things (IoT), and emerging sensing and wearable applications. Recent studies have demonstrated that wideband antenna solutions operating within this frequency range are essential to support high data rates, low latency, and reliable connectivity across multiple communication standards (John et al., 2023). Consequently, a variety of wideband antenna configurations, including conformal antennas, planar patch structures, and coplanar waveguide (CPW)-fed designs, have been proposed to effectively cover large portions of the sub-6 GHz band (Paul et al.,2022; Qui et al.,2020; Sangeetha et al.,2024). However, achieving wide impedance bandwidth while maintaining compact size, stable radiation characteristics, and sufficient gain remains a critical design challenge for sub-6 GHz antenna systems.

Recent research in antenna design has focused on developing compact and efficient radiating structures for modern wireless systems, particularly in the sub-6 GHz and 2.45 GHz bands. For example, Paul et al. proposed a wideband, highly efficient omnidirectional patch antenna targeting WiMAX and lower 5G communications, demonstrating a compact design with high efficiency and broad bandwidth performance suitable for emerging wireless standards (Paul et al.,2023). Similarly, Alkurt et al. introduced a radiation pattern-reconfigurable cubical antenna array optimized for 2.45 GHz indoor wireless applications, emphasizing multidirectional performance through a novel array architecture (Alkurt et al.,2023). These studies highlight ongoing advancements in antenna miniaturization, bandwidth enhancement, and radiation control, supporting the continued exploration of additive manufacturing and novel material integration in antenna fabrication.

Among various wideband radiators, bow-tie antennas have emerged as a highly attractive solution due to their inherently wide impedance bandwidth, planar geometry, and simple radiating structure. As the planar counterpart of conventional biconical antennas, bow-tie configurations enable broadband operation by supporting smoothly distributed surface currents along their flared arms, thereby avoiding narrow resonant behavior. Owing to these characteristics, bow-tie antennas have been widely investigated for navigation, radar, and broadband communication systems where stable radiation performance over a wide frequency range is required (Chen et al.,2017). Recent studies have further demonstrated that bow-tie-based radiators can be adapted to different wideband architectures, including circularly polarized designs, endfire configurations, and array topologies, through appropriate modifications in geometry and feeding mechanisms (Sun et al.,2018; Li et al.,2016).

Despite their broadband advantages, bow-tie antennas typically suffer from limited realized gain due to their distributed radiation mechanism and quasi-omnidirectional radiation characteristics. In many sub-6 GHz wireless, radar, and sensing applications, sufficient gain is essential to improve link budget, signal-to-noise ratio, and radiation coverage. Therefore, effective gain enhancement techniques that preserve wideband behavior while maintaining compact size remain an important research topic for bow-tie antenna systems.

This work presents a wideband bow-tie antenna operating in the sub-6 GHz band, followed by a systematic gain enhancement approach through the integration of a reflector structure fabricated using additive manufacturing technology. The antenna is first designed and experimentally characterized in its standalone configuration and subsequently combined with a 3D-printed reflector to enable a quantitative investigation of gain enhancement and radiation behavior.

## 2. Literature Survey

In the literature, various techniques have been employed to increase the gain of wideband antennas that inherently exhibit low gain. The proposed techniques have their own advantages and disadvantages in terms of bandwidth performance, structural complexity, and fabrication requirements.

To address the gain limitation of wideband antennas, reflector-based techniques have been extensively employed as an effective and structurally simple solution. In particular, the integration of reflectors or cavity-backed structures with wideband bow-tie antennas has been shown to enhance radiation control and realized gain without significantly compromising impedance bandwidth (Yang et al.,2015). Metallic reflectors and cavity-backed configurations have been reported to improve antenna directivity, suppress backward radiation, and reduce sidelobe levels, leading to substantial gain enhancement across a wide range of frequency bands (Yusuf et al.,2018). Such reflector-assisted designs have been successfully applied from microwave radar systems to millimeter-wave antennas, where radiation efficiency and pattern control are critical (Ameya et al.,2018; Zhao et

al.,2019; Li et al., 2020). Recent advances in additive manufacturing have introduced new opportunities for antenna and reflector fabrication, enabling lightweight structures, geometric flexibility, and customizable electromagnetic properties. In this context, RF-optimized dielectric materials such as PREPERM ABS filament have attracted increasing attention for 3D-printed antenna applications. Experimental studies in (Dokmetas et al.,2026) demonstrated that PREPERM ABS can be effectively utilized in a 3D-printed cylindrical dielectric antenna, achieving stable dual-band operation in the X- and Ku-bands with measured realized gains exceeding 6 dBi. Similarly, a PREPERM-based 3D-printed microstrip antenna for WiFi backscatter communication reported in (Onay et al., 2025) achieved high radiation efficiency and notable gain improvement compared to conventional RFID-based designs, confirming the low-loss and repeatable RF performance of the material. In contrast, several recent studies have focused primarily on simulation-based investigations of additively manufactured antenna concepts without proceeding to physical fabrication (Dokmetas et al.,2024; Dokmetas et al.,2023). While these works highlight the electromagnetic performance potential and geometric flexibility offered by additive manufacturing, experimental validation of reflector-assisted wideband antenna systems remains limited. Consequently, there exists a clear research gap in experimentally validated, reflector-backed wideband bow-tie antennas that combine additive manufacturing with RF-optimized dielectric materials to achieve simultaneous wide bandwidth and enhanced gain in the sub-6 GHz frequency range.

## 3. Material and Method

The proposed bow-tie antenna is based on a novel crossed triangular geometry composed of two nested equilateral triangles, which are symmetrically arranged on both the top and bottom surfaces of the dielectric substrate. This configuration is deliberately selected to enhance wideband behavior while preserving structural simplicity and geometric coherence. The use of nested equilateral triangles enables multiple effective current paths of different electrical lengths, allowing the antenna to support broadband impedance characteristics without relying on complex matching networks or multilayer metallic structures. Compared to conventional single bow-tie or planar triangular antennas, the crossed and nested triangular topology provides improved current distribution continuity and mitigates abrupt resonance behavior, which is particularly beneficial for stable operation across the sub-6 GHz frequency range.

The antenna is fabricated on a dielectric substrate realized using PREPERM ABS800 filament, which is specifically engineered for RF and microwave applications. The substrate is manufactured via fused deposition modeling (FDM) with a controlled infill ratio of 55%, resulting in an effective relative permittivity of $\varepsilon_r \approx 4.3$ and a substrate thickness of 1.7 mm. To further enhance electromagnetic symmetry and radiation stability, the same crossed triangular geometry is implemented on both sides of the substrate in a mirror-symmetric manner. This bilateral arrangement not only improves impedance consistency but also contributes to balanced radiation characteristics by maintaining symmetry in surface current excitation. The combination of the nested equilateral triangular bow-tie structure with a precisely controlled 3D-printed PREPERM substrate forms the foundation of the proposed antenna design, enabling a compact, broadband, and fabrication-friendly solution suitable for sub-6 GHz wireless and sensing applications. Figures 1 and Figure 2 presents the frequency-dependent dielectric constant and loss tangent characteristics of different PREPERM ABS materials over a wide frequency range. As observed in Figure 1, the relative permittivity values remain highly stable with negligible dispersion across the investigated frequencies, indicating consistent dielectric behavior suitable for broadband antenna applications. Figure 2 shows that the loss tangent values of all PREPERM ABS variants remain below 0.004 throughout the frequency range, confirming low-loss performance at microwave frequencies. These material characteristics demonstrate that PREPERM ABS filaments provide stable and predictable electromagnetic properties, making them well suited for additively manufactured RF and antenna structures.

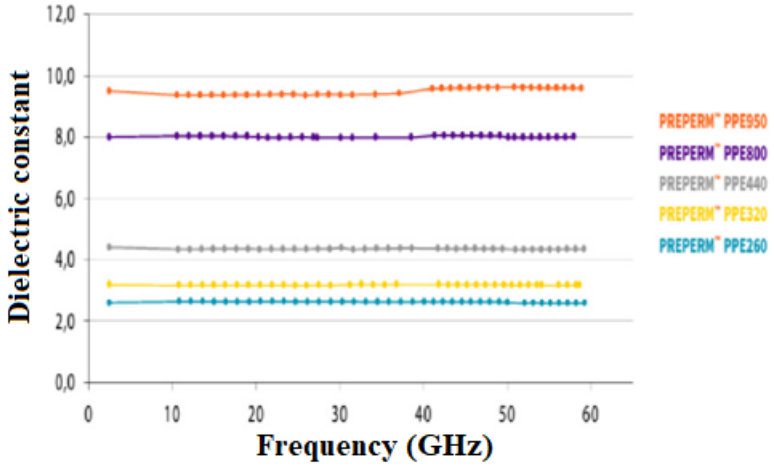


**Figure 1.** Frequency-dependent dielectric constant values of different PREPERM ABS materials

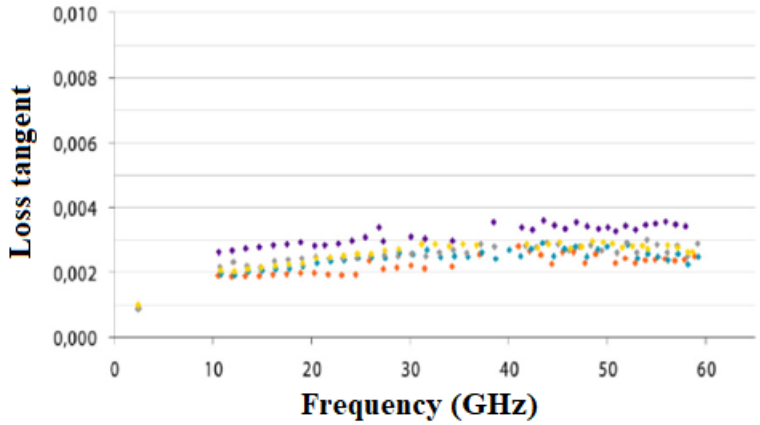


**Figure 2.** Frequency-dependent loss tangent values of different PREPERM ABS materials

Figure 3 illustrates the detailed geometric configuration of the proposed crossed bow-tie antenna, where all critical dimensional parameters are explicitly defined to clarify the design methodology. The antenna consists of two nested equilateral triangular elements forming a crossed bow-tie topology, which enables multiple effective current paths and contributes to broadband impedance behavior. Parameters w3, w4, w5 and w6 define the primary triangular arm dimensions and effective flare lengths, directly influencing the operating bandwidth and resonant behavior of the antenna. The feeding structure is characterized by parameters w1, w2, and w7 which control the excitation balance and impedance matching between the feed line and the radiating elements. This parametrized representation provides a clear framework for systematic optimization and ensures reproducibility of the proposed design. Figure 4 provides a planar projection of the proposed antenna structure, emphasizing the effective radiating aperture formed by the superposition of the nested triangular elements. Rather than representing individual geometric parameters, this view highlights how the crossed bow-tie topology enlarges the electrically active region around the feed point. The overlapping triangular profiles generate a gradual expansion of the current flow area, which effectively increases the aperture size without increasing the overall footprint of the antenna. This distributed aperture formation plays a key role in achieving broadband impedance behavior, as it enables the excitation of multiple resonant modes that smoothly overlap across the operating frequency range.

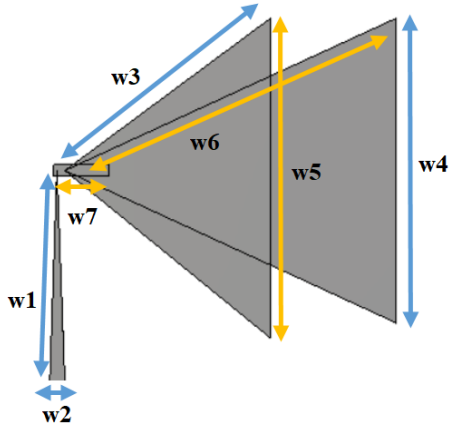


**Figure 3.** Geometry of the proposed crossed bow-tie antenna based on nested equilateral triangular elements

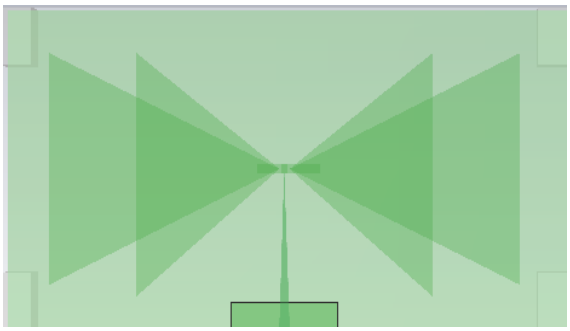

**Figure 4.** Top view of the proposed crossed bow-tie antenna geometry

The feeding line of the proposed bow-tie antenna is designed based on conventional microstrip transmission line theory to achieve proper impedance matching with a standard 50-Ω source. The width of the microstrip feed line is selected according to the effective dielectric constant and substrate thickness to ensure a characteristic impedance close to 50 Ω.

To enhance the realized gain of the proposed bow-tie antenna, a reflector structure is designed and integrated into the antenna system. The reflector is realized using a dielectric substrate with an effective relative permittivity of $\varepsilon_r$ = 4.3 and a thickness of 1.7 mm, which is fabricated using PREPERM ABS800 filament through fused deposition modeling. A copper conductive layer is placed on the bottom surface of the dielectric substrate to form the reflective surface. The reflector is mechanically integrated with the bow-tie antenna by means of four supporting beams located at the corners of the structure, ensuring stable and symmetric spacing between the radiator and the reflector. These supporting beams are also fabricated using PREPERM ABS800 material with a controlled infill ratio of 55%, maintaining dielectric consistency throughout the structure. The proposed reflector configuration provides a compact and fabrication-friendly solution for gain enhancement while preserving the wideband characteristics of the bow-tie antenna.

Figure 5 and Figure 6 illustrate the three-dimensional configuration and geometric integration of the proposed bow-tie antenna with the dielectric-backed reflector structure. As shown in Figure 5, the antenna and reflector are arranged in a vertically separated configuration, where the reflector is positioned beneath the radiating element to redirect backward radiation toward the forward hemisphere. The reflector is mechanically supported by four dielectric beams placed at the corners, ensuring stable alignment and preserving electromagnetic symmetry. Figure 6 further defines the overall reflector dimensions and the separation distance between the antenna and the reflector, denoted by H1, along with the lateral dimensions L1 and L2. This controlled spacing plays a critical role in constructive interference between the directly radiated fields and the reflected waves, leading to enhanced forward gain while maintaining the wideband impedance characteristics of the bow-tie antenna. The overall dimensions of the integrated antenna–reflector structure are 56 mm × 108 mm, with a total height (thickness) of

41.7 mm, as illustrated in the figure. Several antenna–reflector gap distances were investigated during the design process, and the final height of 41.7 mm corresponds to the optimized gap configuration that provided the best overall electromagnetic performance. The spacing between the antenna and the reflector is maintained by four supporting posts, each having a cross-sectional size of 6 mm × 10 mm and a height of 38 mm. Table 1 summarizes the optimized geometrical parameters of the proposed bow-tie antenna and the integrated reflector structure used in the design.

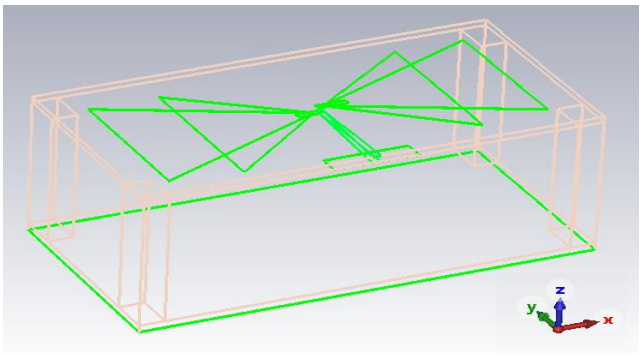


**Figure 5.** Wireframe representation of the proposed bow-tie antenna integrated with the dielectric-backed reflector.

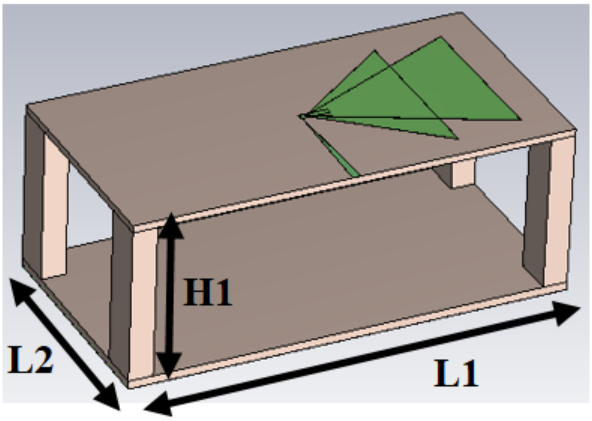


**Figure 6.** Dimensional parameters of the dielectric-backed reflector structure

**Table 1.** Optimized parameters of the proposed bow-tie antenna and reflector

| PARAMETER | VALUE (mm) | PARAMETER | VALUE (mm) |
|---|---|---|---|
| $w_1$ | 28.02 | $w_6$ | 47.8 |
| $w_2$ | 2 | $w_7$ | 7.3 |
| $w_3$ | 33.6 | $L_1$ | 108 |
| $w_4$ | 40 | $L_2$ | 56 |
| $w_5$ | 42 | $H_1$ | 38.04 |

## 4. Simulation and Experimental Results

In this section, the electromagnetic performance of the proposed bow-tie antenna and the integrated reflector configuration is evaluated through both numerical simulations and experimental measurements. The full three-dimensional antenna model is first analyzed using CST Microwave Studio to investigate the reflection coefficient, radiation characteristics, and gain performance across the operating frequency band. Subsequently, a physical prototype of the antenna is fabricated and measured to validate the simulation results. Figure 7 presents a comparative illustration of the $S_{11}$ results obtained throughout the design evolution of the proposed bow-tie antenna. The single triangular configuration demonstrates the wideband behavior of the basic single-triangle structure; however, the impedance matching remains limited in certain frequency regions within the band. When the geometry is transformed into the nested triangular configuration, additional current paths and different effective electrical lengths introduced by the nested triangles give rise to new resonant modes, and the overlap of these modes leads to a noticeable improvement in impedance matching. In the final stage, by adding a reflector beneath the nested triangular structure (reflector-backed), the antenna reflector coupling reshapes the input impedance, resulting in changes in both the resonance depths and their frequency locations. As shown in Figure 7,

the final reflector-backed antenna operates over a frequency range of 1.4–3.9 GHz, corresponding to an effective impedance bandwidth of approximately 2.5 GHz. While the overall wideband characteristic is preserved with the inclusion of the reflector, a more balanced impedance matching behavior is achieved across the operating band, clearly indicating that the impedance bandwidth can be effectively controlled through the proposed geometric and structural modifications.

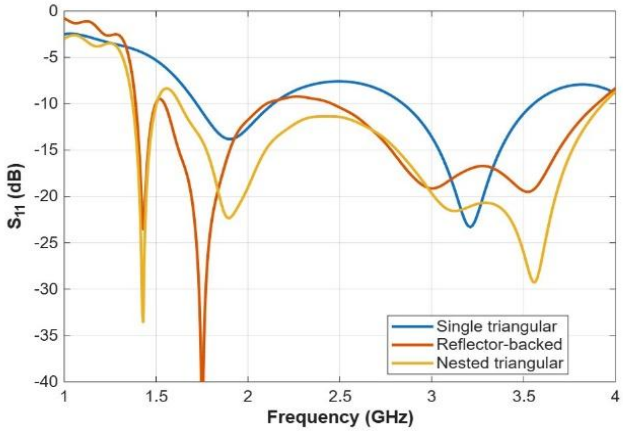


**Figure 7.** Simulated return loss results of the proposed bow-tie antenna configurations

Figure 8 compares the simulated gain performance of the proposed bow-tie antenna with and without the reflector across the operating frequency range. In the absence of the reflector, the antenna exhibits relatively moderate gain values, which gradually increase with frequency due to the electrically larger aperture at higher frequencies. When the reflector is integrated, a clear gain enhancement is observed over the entire band, indicating effective suppression of backward radiation and constructive reinforcement in the forward direction. The maximum gain improvement is achieved around the mid-to-upper frequency region, where the antenna–reflector spacing enables favorable phase alignment between the direct and reflected fields. Within the operating frequency range of 1.4–3.9 GHz, the integration of the reflector leads to a clear and consistent gain enhancement. Without the reflector, the antenna gain increases from approximately 1.5 dBi at 1.5 GHz to about 4.0 dBi around 3.5–3.9 GHz. When the reflector is introduced, the gain is improved to approximately 5.7–5.9 dBi in the lower part of the band and reaches about 5.8 dBi near 3.5 GHz. Overall, the reflector provides an average gain improvement of approximately 1.8–3.0 dB across the effective operating band, confirming its effectiveness in enhancing the forward radiation performance within the intended frequency range.

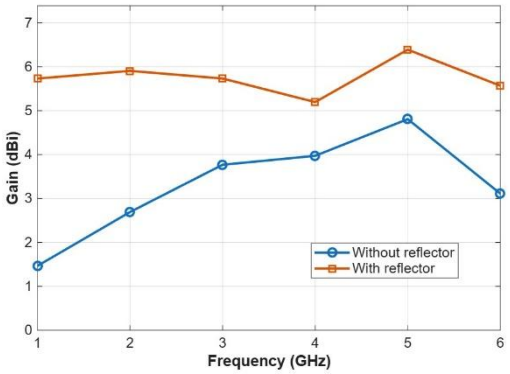


**Figure 8.** The gain performance comparison of the proposed bow-tie antenna with and without the reflector

Figure 9 illustrates the variation of the front-to-back (F/B) ratio of the proposed antenna as a function of frequency. The results show a clear improvement in the F/B ratio across the operating band, with values exceeding 10 dB around the mid-band frequencies, indicating effective suppression of backward radiation. This behavior confirms the role of the reflector in enhancing forward radiation and improving radiation directivity.

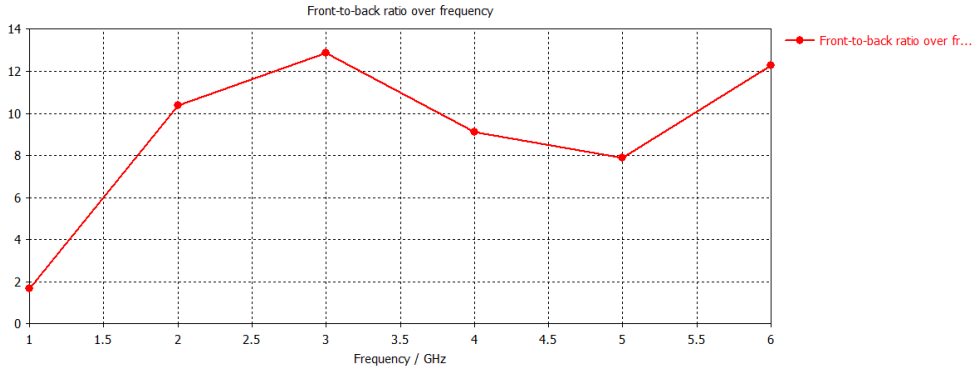


**Figure 9.** Front to back ratio of the proposed structure

Figure 10 illustrates the variation of the reflection coefficient $S_{11}$ of the proposed antenna for different antenna–reflector separation distances. As the gap between the radiator and the reflector changes, noticeable shifts in resonance frequencies and matching levels are observed, indicating the strong influence of antenna-reflector coupling on the input impedance. Smaller separation distances result in deeper resonances at lower frequencies due to stronger near-field interaction, whereas increasing the gap leads to resonance shifts toward higher frequencies and a redistribution of the impedance bandwidth. As the gap increases from 10 mm to 40 mm, the impedance matching significantly improves over a wide portion of the band, with the minimum $|S_{11}|$ level deepening from approximately −18 dB to below −40 dB around 1.8 GHz. In addition, larger gap values lead to a more pronounced resonance behaviour in the lower-frequency region, whereas smaller gaps result in shallower $|S_{11}|$ minima and slightly degraded matching, particularly above 5 GHz.

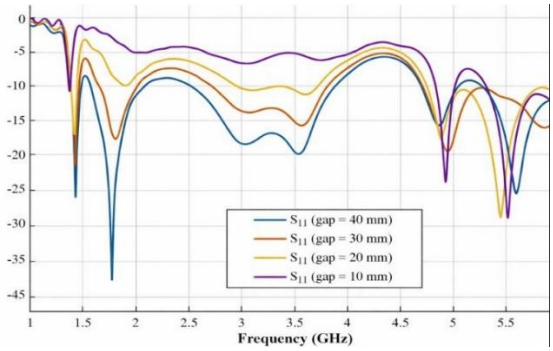


**Figure 10.** Effect of the gap (between antenna and reflector) on the reflection coefficient

Figure 11 (a–c) present the three-dimensional realized gain radiation patterns of the proposed bow-tie antenna at 2 GHz (a), 3 GHz (b), and 4 GHz (c). In all cases, the antenna exhibits a stable radiation behavior with dominant radiation toward the broadside direction and a nearly symmetric pattern distribution. The similarity of the main lobe orientation and overall radiation shape across the examined frequencies confirms that the proposed bow-tie geometry maintains consistent radiation characteristics over the operating band. According to the simulation results, the proposed antenna achieves realized gain values of 2.64 dBi at 2 GHz, 3.72 dBi at 3 GHz, and 3.34 dBi at 4 GHz, further confirming stable radiation performance across the investigated frequency band.

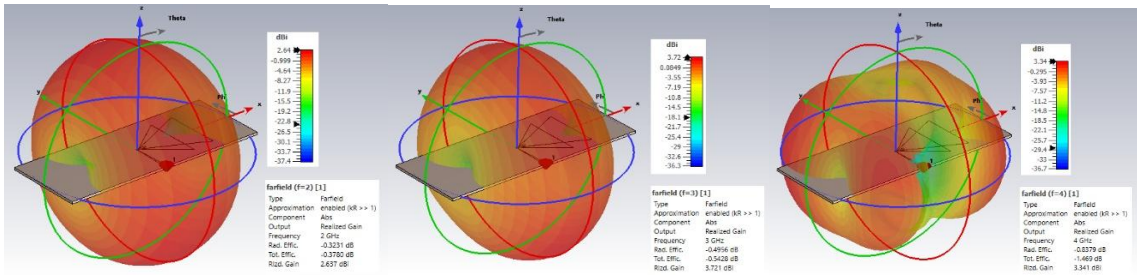

(a) (b) (c)

**Figure 11.** 3D radiation patterns of the proposed bow-tie antenna without reflector at (a) 2 GHz, (b) 3 GHz, and (c) 4 GHz

Figure 12 (a–c) illustrate the three-dimensional realized gain radiation patterns of the proposed bow-tie antenna with the integrated reflector at 2 GHz (a), 3 GHz (b), and 4 GHz (c). Compared to the reflector-free case, the radiation patterns exhibit a more directive behavior with a pronounced enhancement in the forward radiation region. The presence of the reflector effectively redistributes the radiated power toward the broadside direction, leading to improved directivity and reduced radiation toward the opposite hemisphere. The consistent main lobe orientation across the examined frequencies indicates stable radiation characteristics over the operating band. With the inclusion of the reflector, the simulation results indicate that the realized gain increases to 5.61 dBi at 2 GHz, 5.68 dBi at 3 GHz, and 4.50 dBi at 4 GHz, demonstrating a clear enhancement in radiation performance across the operating band.

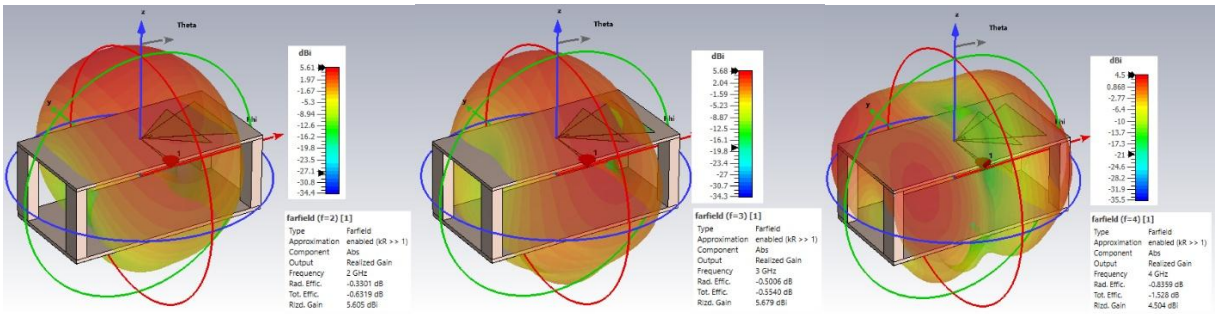


(a) (b) (c)

**Figure 12.** 3D radiation patterns of the proposed bow-tie antenna with reflector at (a) 2 GHz, (b) 3 GHz, and (c) 4 GHz

The antenna and reflector components were fabricated using a Creality CR-5 Pro-H fused deposition modeling (FDM) 3D printer. The printer offers a build volume of 300 × 225 × 380 $mm^3$ and a dimensional accuracy of ±0.1 mm, which is sufficient for reliable fabrication of sub-6 GHz RF structures. During fabrication, a nozzle temperature below 300 °C, a heated build plate below 110 °C, and a layer thickness in the range of 0.1–0.3 mm were employed to ensure dimensional stability and repeatability of the PREPERM ABS800 dielectric parts.The antenna measurements were carried out using a spectrum analyzer as shown in Figure 13 (a) equipped with a tracking generator and an RF bridge, as illustrated in the measurement setup. The tracking generator provides a swept RF excitation signal, which is applied to the antenna under test through the RF bridge. The reflected signal from the antenna is routed back to the spectrum analyzer, enabling the characterization of the antenna response over the frequency band of interest. This configuration allows reliable evaluation of antenna performance in a reflection-reduced measurement environment. Figure 13 (b) shows the top view of the proposed bow-tie antenna. The dielectric substrate and supporting structural components were manufactured in a single fabrication workflow to ensure dimensional accuracy and mechanical stability. After the printing process, the radiating elements were realized by applying the conductive layer onto the printed substrate. This fabrication approach demonstrates the practicality and repeatability of the proposed antenna design for rapid prototyping and experimental validation. Figure 13(c) illustrates the fabricated antenna prototype with the integrated reflector. Measurements were carried out in a reflection-reduced environment using RF absorbing materials. The antenna was positioned within a setup surrounded by RF absorbing materials to reduce the influence of environmental reflections. This measurement configuration aims to provide a reliable verification of the fundamental performance characteristics of the antenna.

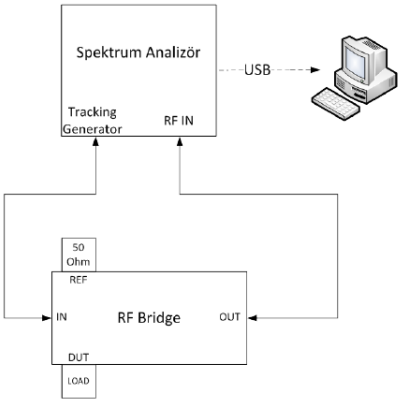


(a)

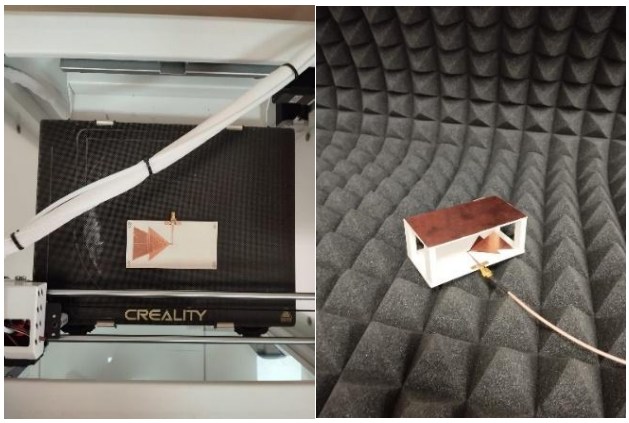


(b) (c)

**Figure 13.** (a) Block diagram of the antenna measurement setup (b) Photograph of the bow-tie antenna top view (c) Side view of the antenna with the reflector

Figure 14 shows the measurement instrument used to record the antenna response during the experimental evaluation. The measurements were carried out using a spectrum analyzer with tracking generator capability, enabling the characterization of the antenna response over the frequency band of interest. This setup was implemented in a reflection-reduced environment to obtain reliable experimental data for validating the simulated performance. According to the measurement results, the antenna operates over a frequency range from 1.2 GHz to 3.1 GHz, corresponding to an absolute bandwidth of 1.9 GHz.

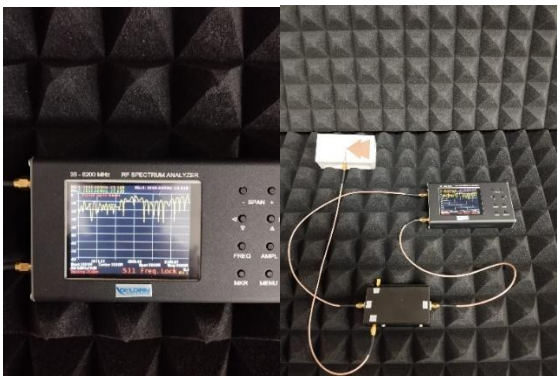

**Figure 14.** Experimental measurement setup using tracking spectrum analyzer

## 5. Conclusion

This study presented a wideband bow-tie antenna operating in the sub-6 GHz band based on a crossed geometry formed by nested equilateral triangular elements and fabricated using a 3D-printed PREPERM ABS800 dielectric

substrate. To enhance the realized gain, a dielectric-backed reflector was integrated and its impact on impedance matching, gain performance, and radiation characteristics was systematically investigated. Simulation and measurement results demonstrated that the nested triangular configuration improves impedance bandwidth, while the reflector provides consistent broadband gain enhancement without degrading wideband operation. The proposed antenna design offers a compact, fabrication-friendly, and practical solution for wireless and sensing applications, highlighting the effectiveness of additive manufacturing techniques in modern antenna engineering. Future research may focus on extending the proposed reflector-backed bow-tie architecture to multi-element array for advanced sub-6 GHz systems.

## Conflict of Interest

No conflict of interest was declared by the authors.

## References


Alkurt, F.O., Unal, E., Palandoken, M., 2023. Radiation pattern reconfigurable cubical antenna array for 2.45 GHz wireless communication applications. Wireless Netw, 29, 235–246.

Ameya, M., Matsukawa, S., Kurokawa, S., 2018. Antenna Gain Self-Calibration Method with Moving Flat Reflector for Millimeter-Wave Frequency Band. IEEE Conference on Antenna Measurements & Applications (CAMA), Vesterås, Sweden, 1–4.

Chen, Y., Li, G., Liu, P., Bian, L., Yi, B., 2017. Wideband, Circularly Polarized, Crossed Bowtie Dipole Antenna for Navigation Satellite System. IEEE 2nd Advanced Information Technology, Electronic and Automation Control Conference (IAEAC), Chongqing, China, 2649–2652.

Dokmetas, B., 2026. 3D-Printed Cylindrical Dielectric Antenna Optimized Using Honey Bee Mating Optimization. Electronics, 15, 393.

Dokmetas, B., Arican, G.O., 2023. Design of Dual-Band SIW Antenna for Millimeter-Wave Communication. 31st Telecommunications Forum (TELFOR), Belgrade, Serbia, 1–4.

Dokmetas, B., Arican, G.O., Yilmaz, B.A., 2024. A Folded Pyramid-Shaped Microstrip Antenna with Improved Bandwidth. IEEE International Symposium on Antennas and Propagation and INC/USNC-URSI Radio Science Meeting (AP-S/INC-USNC-URSI), Florence, Italy, 1273–1274.

John, D.M., Ali, T., Vincent, S., Pathan, S., Kumar, P., 2023. A Conformal Wideband Antenna for Wearable Applications at Sub-6 GHz: Characteristic Mode Analysis. International Telecommunications Conference (ITC-Egypt), Alexandria, Egypt, 29–33.

Kumar, K.M., Sangeetha, M.J., Afrin, S., Gopal, S., Nithin, M.M., Dwivedi, A.K., 2024. Defected Ground Plane Circularly Polarized Wideband Antenna for Sub-6 GHz n77/n78 Application. IEEE International Conference on Interdisciplinary Approaches in Technology and Management for Social Innovation (IATMSI), Gwalior, India, 1–4.

Li, C., Zheng, Y., Sun, Z., Yao, Z., Liu, L., Liu, T., 2020. A High-Gain and Broadband Dipole Antenna Optimized by Partially Reflective Metasurface. IEEE 3rd International Conference on Electronic Information and Communication Technology (ICEICT), Shenzhen, China, 792–794.

Li, J., Li, L., Zhang, A., Liu, J., Liu, Q.H., 2016. Wideband Two Bowtie Dipole Array Antenna Integrated with a Tapered Balun. 11th International Symposium on Antennas, Propagation and EM Theory (ISAPE), Guilin, China, 16–18.

Onay, M.Y., Dokmetas, B., 2025. 3D Printed Microstrip Antenna for Symbiotic Communication: WiFi Backscatter and Bit Rate Evaluation for IoT. Internet of Things, 32, 101643.

Paul, L.C., Ankan, S.S.A., Rani, T., Karaaslan, M., Hossain, M.N., Al-Gburi, A.J.A., Saha, H.K., Alkurt, F.Ö., 2023. A wideband highly efficient omnidirectional compact antenna for WiMAX/lower 5G communications. International Journal of RF and Microwave Computer-Aided Engineering, 2023, pp. 1–11.

Paul, L.C., Saha, H.K., Roy, T.K., Azim, R., Islam, M.T., 2022. A Wideband Inset-Fed Simple Patch Antenna for Sub-6 GHz Band Applications. International Conference on Innovations in Science, Engineering and Technology (ICISET), Chittagong, Bangladesh, 106–110.

Qiu, B., Li, Y., 2020. Asymmetric CPW-Fed Wideband Circularly Polarized Antenna for Sub-6 GHz Application. IEEE 3rd International Conference on Electronic Information and Communication Technology (ICEICT), Shenzhen, China, 626–628.

Sun, Y., Liu, Y., Yu, Y., Du, Z., 2018. Bowtie Dipole Wideband Endfire Antenna with Out-of-Phase Power Divider. International Applied Computational Electromagnetics Society Symposium – China (ACES), Beijing, China, 1–2.

Yang, Z., Cao, W.P., Li, S.M., Jiang, Y., Yu, X., 2015. Design of Ultra-Wideband Dual-Polarization Bowtie Antenna Arrays with Backed Cavity. IEEE International Conference on Communication Problem-Solving (ICCP), Guilin, China, 556–559.

Yusuf, D.P., Zulkifli, F.Y., Rahardjo, E.T., 2018. Design of Narrow-Wall Slotted Waveguide Antenna with V-Shaped Metal Reflector for X-Band Radar Application. International Symposium on Antennas and Propagation (ISAP), Busan, Korea, 1–2.

Zhao, F., Cheng, Y.J., 2019. A Beamforming Method Based on Multi-Variable Optimization for High-Frequency Wide-Angle-Scan High-Gain Array-Fed Reflector Antenna. IEEE Asia-Pacific Microwave Conference (APMC), Singapore, 679–681.